ARTICLE

OBC
www.rsc.org/obc

# Observed and calculated $^{1}$H- and $^{13}$C-NMR chemical shifts of substituted 5*H*-pyrido[3,2-*a*]- and 5*H*-pyrido[2,3-*a*]phenoxazin-5-ones and of some 3*H*-phenoxazin-3-one derivatives †

**Orlando Crescenzi,[a] Gaetano Correale,[b] Adele Bolognese,[b] Vincenzo Piscopo,[c] Michelangelo Parrilli[b] and Vincenzo Barone*[a]**

[a] *Department of Chemistry, University of Naples "Federico II", Via Cintia, I-80126 Naples, Italy*

[b] *Department of Organic Chemistry and Biochemistry, University of Naples "Federico II", Via Cintia, I-80126 Naples, Italy*

[c] *Centro Interdipartimentale di Metodologie Chimico-Fisiche (CIMCF), University of Naples "Federico II", Via Cintia, I-80126 Naples, Italy*

***Received 2nd February 2004, Accepted 29th March 2004***
***First published as an Advance Article on the web 29th April 2004***

Carbon and proton NMR spectra of several substituted 5*H*-pyrido[3,2-*a*]-, 5*H*-pyrido[2,3-*a*]phenoxazin-5-ones and 3*H*-phenoxazin-3-one derivatives have been assigned, and the experimental chemical shifts have been compared with the results of density functional calculations employing large basis sets. Solvent effects were explored by means of the polarizable continuum method (PCM), while the (limited) side-chain flexibility of the compounds has been addressed by Boltzmann averaging of the computed spectral parameters over different conformational minima. Overall, the calculated shifts reproduce well the experiment results; thus, the computational procedure represents a feasible and useful complement to multidimensional NMR experiments in the assignment process.

## Introduction

Phenoxazinones, benzo and pyridophenoxazinones are linear and angular heterocyclic scaffolds containing the iminoquinone moiety responsible for their redox properties.[1,2]

The first phenoxazinone colouring matters discovered in nature were the ommochromes, a class of photosensitive pigments occurring in arthropods, cephalopods and other invertebrates. The structure of the closely related ommins,[3] which constitute the red–violet fraction of cephalopod eye pigments, is still unknown today.

A number of natural and synthetic antiproliferative compounds also contain the phenoxazinone ring system: indeed, it has been shown that the antineoplastic activity is correlated with the ability of the planar heterocyclic moiety to intercalate into double-stranded DNA. In the actinomycins,[4] an important family of antibiotics produced by actinomycetes, the phenoxazinone skeleton is linked to two pentapeptide chains, while meridine and neoamphimedine[5] contain this pharmacophoric moiety within a polycondensed system.

The pH sensitivity of such well known dyestuffs as orceyn and litmus provides evidence of the high electron mobility in the phenoxazinone ring, and of the large influence exerted by substituent groups on the electronic distribution.

The recent[6,7] discovery of a novel class of powerful antitumor intercalating phenoxazinone derivatives rekindled the interest for this system, which is involved in an array of biochemical roles ranging from the photochemical response of vision pigments[8] to the production of DNA-damaging radicals by antiproliferative drugs.[4]

Pursuing our investigation on the NMR characterization of compounds structurally related to the ommochromes,[9] we have now assigned both the proton and the carbon spectra of several new 5*H*-pyrido[3,2-*a*]phenoxazin-5-one, 5*H*-pyrido-[2,3-*a*]phenoxazin-5-one and 3*H*-phenoxazin-3-one derivatives. Since, to the best of our knowledge, no other report has been published after ours,[9] we felt that further NMR data could be useful for a better characterization of this class of compounds.

The strong substituent sensitivity of the spectra prompted us to use quantum mechanical calculations of chemical shifts to support and integrate the usual NMR assignment protocol. However, the series proved to be a good test case for this procedure for other reasons as well. In the first place, the size of the compounds is such that accurate quantum-mechanical methods, while not trivial, are still applicable. On the other hand, the complex chemical nature of the substituted heterocyclic systems makes the use of alternative chemical shift calculation procedures that rely on empirical correlations far from appealing. While several of the compounds examined exhibit a certain conformational flexibility, this is basically limited to the possibility of different side-chain orientations, and the number of significant conformers is still quite limited. Therefore, extensive conformational explorations, which may easily become a bottleneck in a chemical shift calculation procedure on flexible compounds, were not an issue in this series.

Chemical shift calculations produced estimates for all nuclei: however, the discussion will concentrate on $^{13}$C, since carbon chemical shifts are spread over a much larger spectral window than protons, and are therefore less sensitive to small absolute errors in the computed magnetic shielding. Moreover, carbon chemical shifts are particularly amenable to a Density Functional Theory treatment,[10,11] an approach of much higher computational efficiency than alternative (*e.g.* MP2) correlated methods.

To explore the influence of solvation on the chemical shifts we employed the Polarizable Continuum Method (PCM), which allows accurate and effective computation of solvent effects on a variety of spectral parameters (for a recent review, see ref. 12).

## Results and discussion

In order to assign the $^{13}$C-NMR signals we started with a complete assignment of the $^{1}$H-NMR spectrum, obtained from 1D and 2D experiments (TOCSY, COSY, NOESY); carbon signals

† Electronic supplementary information (ESI) available: $^{1}$H and $^{13}$C NMR data for compounds **1**–**17**. See http://www.rsc.org/suppdata/ob/b4/b401147c/

DOI: 10.1039/b401147c

were then attributed by means of one-bond and long-range $^{1}H$–$^{13}C$ heterocorrelated 2D-NMR spectra (HMQC and HMBC).

To the best of our knowledge, the only previous study on the $^{13}C$ NMR spectra of 3*H*-phenoxazin-3-one derivatives dates back from 1985.[13] In this report the $^{13}C$ assignments were based on comparison with $^{13}C$ data of analogous compounds, and were correlated with semiempirical CNDO/2 charge density calculations; however, the assignments of C-5a and C-10a of compound **1** are swapped with respect to our calculations.

Among the other 3*H*-phenoxazin-3-one derivatives (**2**–**7**) (Scheme 1), only the $^{13}C$ NMR spectrum of compound **4** has already been described,[13] but again the reported data do not exactly match with our experimental and computed assignments. In particular, discrepancies were found for the chemical shifts of C-2, C-5a and C-10a: while two of the resonances reported, at $\delta$ 149.4 and 143.3 ppm, were also present in our spectra (at $\delta$ 149.0 and 143.4 ppm), a signal reported as 147.9 ppm did not occur at all in our $^{13}C$ spectrum, where instead a resonance at 137.2 ppm appeared. Even surmising the presence of a misprint, the assignments we determined for C-2, C-5a and C-10a are still at variance with those of ref. 13, since we find C10a at lower field, followed by C5a and C2: this order corresponds to that observed for the closely related compounds **2** and **3**.

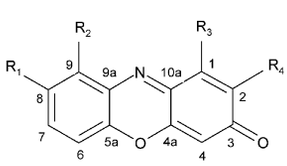

**1** $R_1 = R_2 = R_3 = R_4 = H$
**2** $R_1 = CH_3$; $R_2 = R_3 = R_4 = H$
**3** $R_1 = CH_3$; $R_2 = R_3 = H$; $R_4 = CH_3$
**4** $R_1 = R_2 = R_3 = H$; $R_4 = NHCOCH_3$
**5** $R_1 = H$; $R_2 = R_3 = COCH_3$; $R_4 = NH_2$

**6** $R_1 = H$; $R_2 = R_3 = COCH_3$; $R_4 = Cl$
**7** $R_1 = H$; $R_2 = R_3 = COCH_3$; $R_4 = NHCOCH_3$
**8** $R_1 = H$; $R_2 = R_3 = COCH_2CH(NHCOCH_3)COOCH_3$; $R_4 = NHCOCH_3$
**9** $R_1 = H$; $R_2 = R_3 = COCH_2CH_2COOCH_3$; $R_4 = NHCOCH_3$

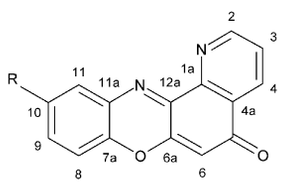

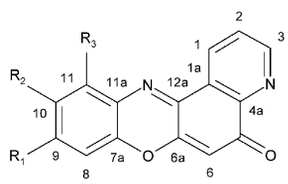

**10** R = H
**11** $R = NO_2$
**12** R = Cl

**13** $R_1 = R_2 = R_3 = H$
**14** $R_1 = R_2 = CH_3$; $R_3 = H$
**15** $R_1 = R_3 = H$; $R_2 = CH(CH_3)CH_2CH_3$
**16** $R_1 = R_2 = H$; $R_3 = CH_3$

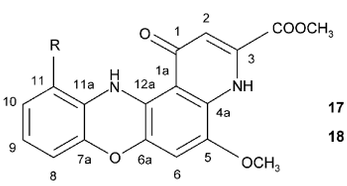

**17** $R = COCH_2CH(NHCOCH_3)COOCH_3$
**18** $R = COCH_3$

**Scheme 1** Chemical formulae and atom numbering of compounds **1**–**18**.

Compounds **5**, **7** and **9**, which carry an acyl substituent at both positions 1 and 9, were examined in order to facilitate the spectral assignment of the natural product **8**, which is available in minute amount.

Carbon and proton isotropic shielding constants were calculated at the Density Functional Theory (DFT) level within the Gauge-Including Atomic Orbitals (GIAO) ansatz.[14] Several recent investigations[15–19] have shown that this approach is best applied to compute relative shieldings, *i.e.* chemical shifts: in consideration of the highly conjugated nature of the systems at hand, we chose as reference compound the benzene molecule (experimental chemical shifts in $CDCl_3$: $\delta_H$ 7.339, $\delta_C$ 128.36 ppm[20]).

For all DFT calculations, we adopted the PBE0 density functional,[21] which has proven particularly reliable for the prediction of magnetic properties,[11,22] with the rather large 6-311+G(d,p) basis set (see ref. 10 for a general discussion of basis sets). Geometry optimizations were also carried out at the DFT (PBE0) level, using the smaller 6-31G(d) basis set.

While it is well known that most hybrid functionals (including PBE0) perform quite similarly in geometry optimization,[21] the choice of the 6-31G(d) basis set was tested on the parent phenoxazone (**1**). When the optimization was repeated with two larger basis sets, 6-31+G(d) and 6-31+G(d,p), the resulting structures were very close to that obtained at the PBE0/6-31G(d) level, with all-atoms root mean square deviations (RMSD) of just 0.003 and 0.002 Å, respectively. Thus, the relatively small size of the 6-31G(d) basis set does not seem to introduce any significant geometrical bias.

In principle, further insight into the quality of the computed geometries can be gained by comparison with experimental (*e.g.* X-ray diffraction) data. Several structures containing the phenoxazinone ring system are present in the Cambridge Structural Database.[23] However, most of them belong to actinomycin derivatives, *i.e.* they carry two cyclized peptides linked through carboxamide groups to positions 1 and 9 of the heterocyclic skeleton. A complete *ab initio* calculation on such large systems, at the same level adopted for our compounds, would be extremely expensive; on the other hand, the influence of the bulky, conjugated substituents on ring geometry would be quite difficult to reproduce in a simplified model.

The only simple compounds of known three dimensional structure appear to be 2-amino-3*H*-phenoxazin-3-one[24] and 2-amino-7-methoxy-3*H*-phenoxazin-3-one.[25] Geometry optimizations of these compounds at the usual PBE0/6-31G(d) level resulted in an agreement with the experimental geometries (RMSD over all bond lengths between heavy-atom of 0.017 and 0.014 Å, respectively) that seems rather satisfactory, especially if one considers that vibrational effects and, more importantly, crystallographic contacts have not been taken into account.

On the other hand, the effect of using different optimized geometries on the computed shifts can be calculated directly. When the PBE0/6-311+G(d,p)//PBE0/6-31G(d) calculation on phenoxazone **1** was repeated at the PBE0/6-31+G(d) and PBE0/6-31+G(d,p) geometries, the RMSDs were 0.22 and 0.21 ppm on all carbon shifts, 0.0087 and 0.0088 ppm on all proton shifts. Thus, it appears that the minor geometrical differences related to the use of larger basis sets do not affect to any significant extent the computed carbon and proton chemical shifts: again, this supports our choice of the 6-31G(d) basis set for geometry optimizations.

Next, we compared the performance of the PBE0 functional with that of the widely used B3LYP for the three parent ring systems, *i.e.* compounds **1**, **10** and **13**. Table 1 shows that the two functionals are essentially equivalent in the prediction of proton shifts, while for carbon shifts the PBE0 results are slightly closer to the experiment, the difference being mostly related to a better agreement for quaternary ring-junction atoms. This is in line with the ability of PBE0 to provide a correct description for carbon atoms in different hybridization states and in a large range of chemical environments.[11,22]

Table 2 shows that adoption of larger basis sets [6-311+G(2d,2p) and 6-311++G(2d,2p)] during the NMR calculations does not significantly improve the agreement with the experimental results.

As a rule, both geometry optimizations and chemical shift calculations were carried out on the isolated molecule *in vacuo*. However, in order to evaluate the influence that the solvent

**Table 1** Comparison of the PBE0 and B3LYP functionals in the prediction of chemical shifts, as judged by RMSDs between experimental and computed shifts (ppm). All NMR calculations use the 6-311+G(d,p) basis set at the PBE0/6-31G(d) geometries

| | $^1$H | | $^{13}$C | | | |
|---|---|---|---|---|---|---|
| | PBE0 | B3LYP | PBE0, all | PBE0, ring junction | B3LYP, all | B3LYP, ring junction |
| **1** | — | — | 1.35 | 1.20 | 1.44 | 1.72 |
| **10** | 0.18 | 0.18 | 1.16 | 0.86 | 1.35 | 1.48 |
| **13** | 0.23 | 0.22 | 1.36 | 1.33 | 1.44 | 1.66 |

**Table 2** Basis set convergence in the prediction of chemical shifts, as judged by RMSDs between experimental and computed shifts (ppm). All NMR calculations use the PBE0 functional at the PBE0/6-31G(d) geometries

| | $^1$H | | | $^{13}$C | | |
|---|---|---|---|---|---|---|
| | 6-311+G(d,p) | 6-311+G(2d,2p) | 6-311++G(2d,2p) | 6-311+G(d,p) | 6-311+G(2d,2p) | 6-311++G(2d,2p) |
| **1** | — | — | — | 1.35 | 1.38 | 1.37 |
| **10** | 0.18 | 0.16 | 0.17 | 1.16 | 1.17 | 1.17 |
| **13** | 0.23 | 0.20 | 0.20 | 1.36 | 1.44 | 1.45 |

**Table 3** Effect of PCM on the RMSD between experimental and computed shifts (ppm)

| | $^1$H | | $^{13}$C | |
|---|---|---|---|---|
| | *In vacuo* | In solution (PCM) | *In vacuo* | In solution (PCM) |
| **1** | — | — | 1.35 | 1.22 |
| **10** | 0.18 | 0.12 | 1.16 | 1.15 |
| **13** | 0.23 | 0.14 | 1.36 | 0.93 |

medium (chloroform) can induce on the geometry and on the computed chemical shifts, we examined again the three parent ring systems, both *in vacuo* and in solution, using an advanced version[26] of the polarizable continuum model (PCM),[27] which besides providing energies and electronic properties allows geometry optimizations and force constant calculations. In the PCM computations, the solvent is represented by a dielectric medium, polarized by the presence of the solute, which in turn exerts a reaction field on the solute charge distribution.[27] The method is described in detail elsewhere: here we shall just recall that in this approach the solute is enclosed in a cavity, with the relative dielectric constant taking a value of 1 within the cavity (*i.e.* the *in vacuo* value), and the solvent bulk value outside (4.9 for chloroform). The cavity is made up by the envelope of spheres centered on solute atoms (or atomic groups); sphere radii have been parameterized to reproduce the solvation free energies of a number of organic and inorganic compounds;[28] for computational reasons, the cavity surface is subdivided analytically into a pattern of small tiles (tesserae).

As expected, introduction of the PCM affords a better agreement between experimental and computed spectra, as measured in terms of RMSD between chemical shifts (Table 3). Overall, however, the computed solvent-induced shifts ($\Delta\delta$) are rather small, reflecting the moderately polar character of the solutes and the solvent used; therefore a generalized adoption of the more expensive PCM model was deemed unnecessary in the present case.

Fig. 1 shows the correlation between all computed and measured chemical shifts of **1**, **10** and **13**: a linear fitting has been often used in the interpretation of such plots, and in a way the introduction of two adjustable parameters is bound to make the agreement between computed and measured shifts better. However, use of an appropriate reference compound for chemical shift calculations makes this procedure unnecessary in the current instance since the slopes of the plots in Fig. 1 are very close to 1.

With the exception of the parent heterocyclic systems (**1**, **10** and **13**), most of the compounds investigated can, at least in principle, give rise to conformational equilibria among different minima. The interconversion between different conformers must be fast on the chemical shift time-scale, since a single set of signals was invariably observed; under these conditions, the observed spectrum is the population-weighted average of the spectra of the individual conformers. Therefore, prior to chemical shift calculation, a conformational exploration was necessary. This was performed by means of unrestrained optimizations, whereby the starting conformations were generated by a systematic combination of the side-chain arrangements expected on the base of chemical intuition. Thus, for example, compound **6** was minimized starting from 10 different conformations, which were built up by combining 4 conformations (2 slightly distorted s-*cis* and two slightly distorted s-*trans* arrangements) for each of the two acetyl groups, and keeping only one member of the resulting pairs of mirror-image starting structures; the remaining two starting structures had both acetyl groups perpendicular to the heterocyclic ring. Only in the case of the larger compounds, for the sake of computational efficiency, a preliminary conformational search was carried out at the HF/3-21G level, and the resulting minima were reoptimized afterwards at the usual PBE0/6-31G(d) level. At any rate, when the exploration revealed the presence of several energetically close minima, spectral parameters were computed for each of them, and eventually combined after Boltzmann weighting to give an estimate of the average shifts. The relative energies of the conformers which entered into the computation of the Boltzmann factors were those of the PBE0/6-311+G(d,p)// PBE0/6-31G(d) calculation.

It may be worthwhile to examine in more detail the results for compound **6**, which was a problematic case in a couple of respects. When computed with the usual protocol, the chemical shifts of H-8 (8.56 ppm) and of C-9 (134.9) were unusually far from the measured values of 7.67 and 139.8 ppm, respectively, while the computed shift of C-8 was just fair (129.5 *vs.* 126.0 ppm). We reasoned that the torsion of the C-9 acetyl group out of the average ring plane could affect these shieldings significantly, and therefore carried out a relaxed geometry scan at the PBE0/6-31G(d) level, with single point energies computed at the PBE0/6-311+G(d,p) level. The results (Fig. 2), supported by free minimizations starting from the scan geometries, show that the single minimum (C-10–C-9–C carbonyl–C methyl dihedral = −10°) found at the lower theory level is replaced at the higher level by a double well, whereby the preferred acetyl conformation is about 45° out of the ring plane. When these more accurate geometries were used for the chemical shift calculation, the agreement with experiment was much better (H-8 at 7.95 ppm, C-9 at 140.2 ppm, C-8 at 128.1 ppm). This emphasizes the fact that stiff parameters (bond lengths and valence angles) are well reproduced at the 6-31G(d) level,

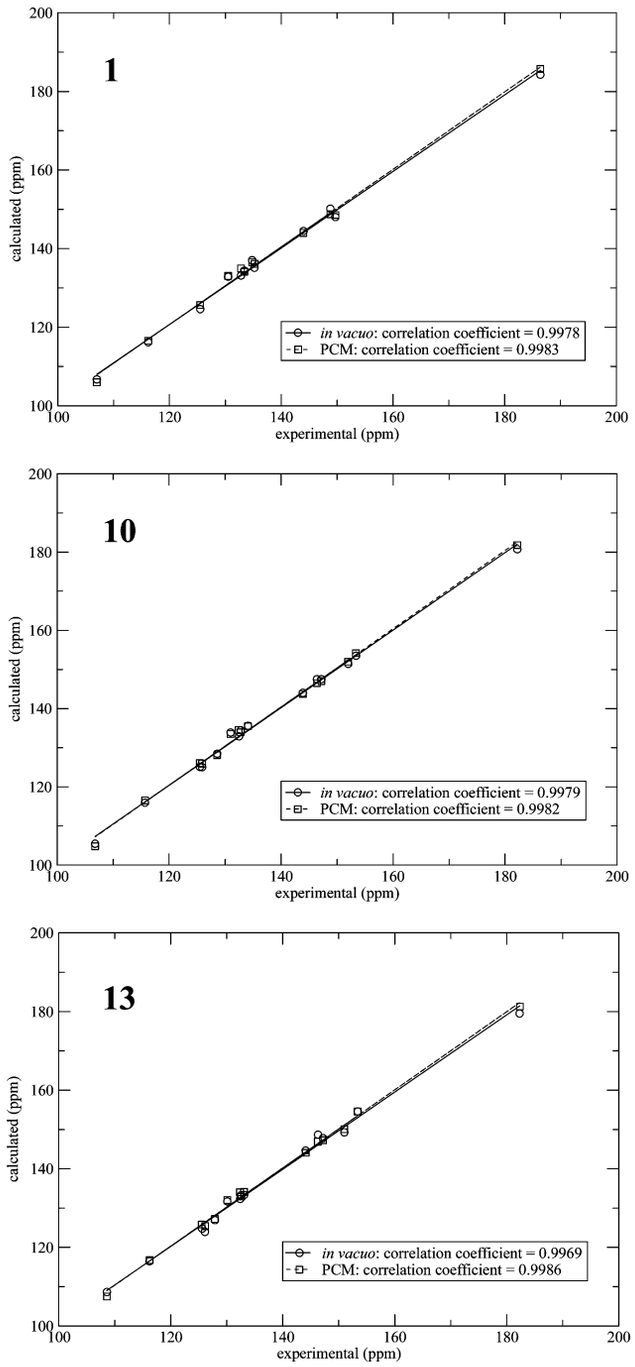


**Fig. 1** Calculated *versus* experimental carbon shifts for the three parent ring systems, compounds **1**, **10** and **13**, both *in vacuo* and in the presence of a polarizable solvent model (PCM).

whereas in some cases soft parameters (torsions) may require a deeper investigation by a larger basis set.

Another issue, apparently unrelated to the former, is the computed chemical shift of the chlorine-bearing carbon, C-2, which is off by as much as 8 ppm (143.2 *vs.* the observed 135.0 ppm). An inaccurate torsion of the C-1 acetyl does not seem to be the problem here: essentially the same acetyl geometry is found at the PBE0/6-31G(d) and PBE0/6-311+G(d,p)//PBE0/6-31G(d) level (Fig. 3); moreover, the influence of the C-1 acetyl torsion on the computed C-2 chemical shift is rather small, and values averaged over the potential energy well are only marginally different from those computed on the most stable conformer. As a matter of fact, even for the simple chlorobenzene molecule the computed chemical shift of the C-1 carbon (141.5 ppm) does not match very well the experimental value (134.33 ppm, in $CDCl_3$[20]), while the remaining carbon shifts are reproduced to within 0.8 ppm. Introduction of the continuum

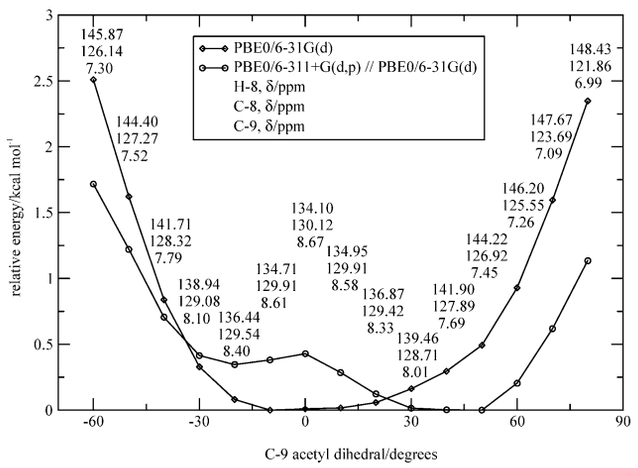


**Fig. 2** Relative energies and selected computed shifts *versus* C-9 acetyl dihedral for compound **6**.

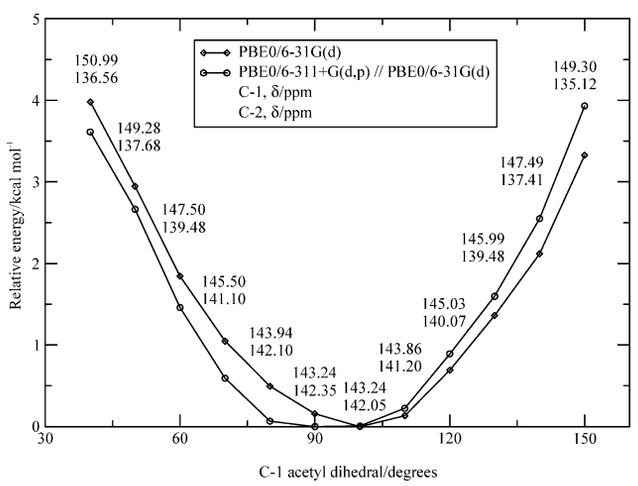


**Fig. 3** Relative energies and selected computed shifts *versus* C-1 acetyl dihedral for compound **6**.

solvent model, use of more accurate geometries [PCM/PBE0/6-311+G(d,p)], and of larger bases during the shift calculation [PCM/PBE0/6-311++G(2d,2p)] alleviated the problem, but did not solve it; even at the MP2 level the C-1 chemical shift of chlorobenzene is the least accurately predicted. It is interesting to note that a similar, although much larger, difference between computed and observed chemical shifts has been recently reported for some bromobenzene derivatives,[19] and has been traced back to a relativistic electronic spin–orbit coupling, which is obviously not taken into account during standard DFT calculations. From a practical viewpoint, of course, one can use the C-1 chemical shift of chlorobenzene itself as the reference for chlorine-bearing carbons, and obtain a nice agreement for the C-2 shift of compound **6** (136.0 ppm *vs.* the observed 135.0 ppm).

## Conclusions

Some more general considerations concerning the use of *ab initio* chemical shift calculations for the assignment of NMR spectra of organic molecules may be drawn from the present results. In the first place, within a given class of compounds (in our case, a series of related heterocyclic rings with different substitutions), the agreement of computed carbon shifts with experimental results is usually to within a couple of ppm's. This means that in favourable cases, *i.e.* when the separation of the signals is sufficiently high with respect to this uncertainty, the computed shifts can be used to assign an experimental carbon spectrum without ambiguity; conversely, when groups of carbon shifts fall very close to each other, the calculation

may not reproduce their correct ordering, so these cases should be treated with caution. Overall, the situation is less favourable for protons, where the reduced spectral dispersion makes even a small (a couple of tenths of ppm) error comparatively significant: however, interpretation of heterocorrelated spectra (and thus proton assignment) is definitely easier when the set of computed carbon and proton shifts is available. Using DFT methodologies, and with appropriate choice of basis sets, a single geometry optimization/shielding calculation on a molecule of the size considered here is not unduly expensive, and is definitely within the reach of the non specialist. Unfortunately, the computational burden increases in proportion with the conformational flexibility of the compound; moreover, a direct exploration of the conformational space in search of all significant energy minima implies a certain dose of chemical intuition, and overall the whole procedure is much less amenable to standardization. In the case of compounds with much larger flexibility than the ones considered here, alternative, more expensive search algorithms need to be considered, and recourse to semiempirical methods, or even classical force fields, during this phase might become necessary. However, the procedure we adopted in the present study is already applicable as such to provide significant aid in the assignment of the NMR spectra of a large array of compounds of interest in synthetic and natural products organic chemistry.

## Experimental

NMR spectra were acquired on Bruker AC-270 and DRX-400 spectrometers, operating at 270 and 400 MHz proton Larmor frequencies, respectively. Pulse programs for the homonuclear (COSY, TOCSY and NOEST) and heteronuclear (HMQC and HMBC) 2D experiments were taken from the standard Bruker library. Quantum-mechanical calculations were performed with the Gaussian package.[29] Compounds **1**–**17** were prepared as described.[6,7]

## Acknowledgements

The technical support of the Centro Interdipartimentale di Metodologie Chimico-Fisiche (CIMCF) and the financial support of the Italian Ministry for University and Research (MIUR) are gratefully acknowledged.

## References

1 W. Schaefer, *Prog. Org. Chem.*, 1964, **6**, 135.
2 M. Ionescu and H. Mantsch, *Adv. Heterocycl. Chem.*, 1967, **8**, 83.
3 G. Prota, in *Marine Natural Products: Chemical Biological Perspectives*, ed. P. J. Scheuer, Academic Press, New York, 1980, vol. 3, p. 141.
4 B. A. Chabner, C. J. Allegra, G. A. Curt and P. Calabresi, in *Goodman and Gilman's The Pharmacological Basis of Therapeutics*, 9th edn., eds. J. G. Hardman, L. E. Limbird, P. B. Molinoff, R. W. Ruddon and A. G. Gilman, McGraw-Hill, NewYork, 1996, p. 1233.
5 E. Delfourne, F. Darro, N. Bontemps-Subielos, C. Decaestecker, J. Bastide, A. Frydman and R. Kiss, *J. Med Chem.*, 2001, **44**, 3275.
6 A. Bolognese, G. Correale, M. Manfra, A. Lavecchia, O. Mazzoni, E. Novellino, V. Barone, A. Pani, E. Tramontano, P. La Colla, C. Murgioni, I. Serra, G. Setzu and R. Loddo, *J. Med Chem.*, 2002, **45**, 5205.
7 A. Bolognese, G. Correale, M. Manfra, A. Lavecchia, O. Mazzoni, E. Novellino, V. Barone, P. La Colla and R. Loddo, *J. Med Chem.*, 2002, **45**, 5217.
8 V. Barone, A. Bolognese and M. Buonanno, *J. Heterocycl. Chem.*, 1995, **32**, 743–746.
9 (*a*) A. Bolognese, G. Scherillo and W. Schaefer, *J. Heterocycl. Chem.*, 1986, **23**, 1003; (*b*) A. Bolognese and M. Parrilli, *Heterocycles*, 1992, **34**, 1829.
10 J. B. Foresman and A. Frisch, *Exploring Chemistry with Electronic Structure Methods*, Gaussian Inc., Pittsburgh, 1998.
11 C. Adamo, M. Cossi and V. Barone, *J. Mol. Struct. Theochem.*, 1999, **493**, 145.
12 V. Barone, O. Crescenzi and R. Improta, *Quant. Struct.-Act. Relat.*, 2002, **21**, 105.
13 K. Hasegawa and Y. Ueno, *Bull. Chem. Soc. Jpn.*, 1985, **58**, 2832.
14 J. R. Cheesman, G. W. Trucks, T. A. Keith and M. J. Frisch, *J. Chem. Phys.*, 1998, **104**, 5497.
15 M. J. Allen, W. K. Thomas and D. J. Tozer, *Chem. Phys. Lett.*, 2003, **380**, 70.
16 G. Barone, L. Gomez-Paloma, D. Duca, A. Silvestri, R. Riccio and G. Bifulco, *Chem. Eur. J.*, 2002, **8**, 3233.
17 M. Cossi and O. Crescenzi, *Theor. Chem. Acc.*, 2004, **111**, 162.
18 E. Fadda, M. E. Casida and D. R. Salahub, *J. Phys. Chem. A*, 2003, **107**, 9924.
19 A. Bagno, F. Rastrelli and G. Saielli, *J. Phys. Chem. A*, 2003, **107**, 9964.
20 Integrated Spectral Data Base System for Organic Compounds: http://www.aist.go.jp/RIODB/SDBS/menu-e.html.
21 C. Adamo and V. Barone, *J. Chem. Phys.*, 1999, **110**, 6158.
22 C. Adamo and V. Barone, *Chem. Phys. Lett.*, 1999, **298**, 113.
23 F. H. Allen, S. Bellard, M. D. Brice, B. A. Cartwright, A. Doubleday, H. Higgs, T. Hummelink, B. G. Hummelink-Peters, O. Kennard, W. D. S. Motherwell, J. R. Rodgers and D. G. Watson, *Acta Crystallogr. Sect. B*, 1979, **35**, 2331.
24 J. Nie and D. Xu, *Jiegou Huaxue*, 2002, **21**, 165.
25 R. G. Buckley, J. Charalambous and K. Henrick, *Acta Crystallogr. Sect. B*, 1982, **38**, 289.
26 M. Cossi, G. Scalmani, N. Rega and V. Barone, *J. Chem. Phys.*, 2002, **117**, 43.
27 J. Tomasi and M. Persico, *Chem. Rev.*, 1994, **94**, 2027.
28 V. Barone, M. Cossi and J. Tomasi, *J. Chem. Phys.*, 1997, **107**, 3210.
29 M. J. Frisch, G. W. Trucks, H. B. Schlegel, G. E. Scuseria, M. A. Robb, J. R. Cheeseman, J. A. Montgomery, Jr., T. Vreven, K. N. Kudin, J. C. Burant, J. M. Millam, S. S. Iyengar, J. Tomasi, V. Barone, B. Mennucci, M. Cossi, G. Scalmani, N. Rega, G. A. Petersson, H. Nakatsuji, M. Hada, M. Ehara, K. Toyota, R. Fukuda, J. Hasegawa, M. Ishida, T. Nakajima, Y. Honda, O. Kitao, H. Nakai, M. Klene, X. Li, J. E. Knox, H. P. Hratchian, J. B. Cross, C. Adamo, J. Jaramillo, R. Gomperts, R. E. Stratmann, O. Yazyev, A. J. Austin, R. Cammi, C. Pomelli, J. W. Ochterski, P. Y. Ayala, K. Morokuma, G. A. Voth, P. Salvador, J. J. Dannenberg, V. G. Zakrzewski, S. Dapprich, A. D. Daniels, M. C. Strain, O. Farkas, D. K. Malick, A. D. Rabuck, K. Raghavachari, J. B. Foresman, J. V. Ortiz, Q. Cui, A. G. Baboul, S. Clifford, J. Cioslowski, B. B. Stefanov, G. Liu, A. Liashenko, P. Piskorz, I. Komaromi, R. L. Martin, D. J. Fox, T. Keith, M. A. Al-Laham, C. Y. Peng, A. Nanayakkara, M. Challacombe, P. M. W. Gill, B. Johnson, W. Chen, M. W. Wong, C. Gonzalez and J. A. Pople, Gaussian 03, Gaussian Inc., Pittsburgh, 2003.